# PRELIMINARY INVESTIGATION OF FRICTION STIR WELDING ALUMINIUM/COPPER LAP JOINTS

**A. Elrefaey[1], M. Takahashi[2], K. Ikeuchi[2]**
**[1] Graduate School of Osaka University**
**[2] Joining and Welding Research Institute, Osaka University**
**(Japan)**

## ABSTRACT

An investigation has been made of the feasibility of friction stir welding of dissimilar lap joint of an aluminium plate to a copper plate, which is difficult to weld by fusion welding methods because of the formation of brittle intermetallic compounds (IMC). Although the level of bond strength was quite low, it exhibited a general tendency to increase with a rise in rotation speed. Various microstructures with different morphologies and properties were observed in the stirred zone of aluminium and Al/Cu interfacial region. Comparison of the fracture location with the microstructure suggests that IMC formed in the interfacial region was responsible for the low strength of the joints. X-ray diffraction from the fracture surfaces indicate that $Al_4Cu_9$, AlCu, and $Al_2Cu$ were the main intermetallic compounds formed in the interfacial region. The performance of the joints was improved significantly by using Zn intermediate layer between Al and Cu owing to limiting the formation of the harmful intermetallic compounds and distributing them over wider areas.

***IIW-Thesaurus keywords:*** *Friction stir welding; Friction welding; Lap joints; Aluminium; Light metals; Copper; Zinc; Peel tests; Mechanical tests; Mechanical properties; Reference lists.*

## 1 INTRODUCTION

To meet the requirements from the electric industry the joining of aluminium to copper have been carried out by many methods such as ultrasonic welding [1], friction welding [2], and laser welding [3]. The major difficulty in the fusion welding of aluminium to copper is the occurrence of brittle intermetallic compounds in the joint zone.

Over the last decade, on the other hand, friction stir welding (FSW) has offered a great welding quality to the joint of aluminium, magnesium [4], titanium [5], copper [6], and steel [7-9]. Recently, some trials have been made to join dissimilar materials, for examples, dissimilar Al alloys [10] and aluminium-to-steel [11-14].

A few preliminary studies have also been reported for the FSW of aluminium-to-copper (Al-Cu) butt joint [15-17], but as far as we know, no investigation of FSW of Al-Cu lap joints with the aid of an intermediate layer has been reported. The present research has been aimed at investigating the phenomena occurring at the interface during FSW of Al-Cu lap joint with and without zinc (Zn) intermediate layer, and discussing the effect of the intermediate layer on the performance of the joint.

Doc. IIW-1662-04 (ex-doc. IX-2105-04) recommended for publication by Commission IX “Behaviour of metals subjected to welding”.

## 2 EXPERIMENTAL

A plate of commercially pure aluminium A1100H24 2.0 mm thick was friction-stir-welded to a plate of tough pitch copper of 99.96 %, 1.0 mm in thickness. A zinc foil of 50 µm thickness was employed as an intermediate layer. The chemical composition of the aluminium plate is listed in Table 1. The microstructures of the base metals are shown in Figure 1. The aluminium base metal showed elongated grains in the rolling direction as shown in Figure 1 (a). The copper base metal presented recrystallised grains as indicated in Figure 1 (b).

Rotation and travel speeds of the FSW tool employed in welding with and without an intermediate layer were listed in Table 2. Weld No. from 1 to 12 represented the joints without a Zn intermediate layer, while weld No. 13 and 14 represented the joint welded with a Zn intermediate layer. The depth of the pin tip from the upper surface of the aluminium plate was fixed at 2.1 mm in welding without intermetallic layer and at 2.2 mm in welding with Zn intermediate layer (50 µm thick).

The tool of steel SKD61 was comprised of a shank, shoulder and pin [18]. The tool axis was tilted by 3° with respect to the vertical axis of the plate surface. The FSW tool, fixed in the holder, was slowly pushed into the

**Table 1 – Chemical composition of the aluminium base metal 1100H24 (mass %)**

| Si | Fe | Cu | Mn | Mg | Ti | Al |
|---|---|---|---|---|---|---|
| 0.12 | 0.54 | 0.12 | 0.01 | 0.03 | 0.03 | Bal. |

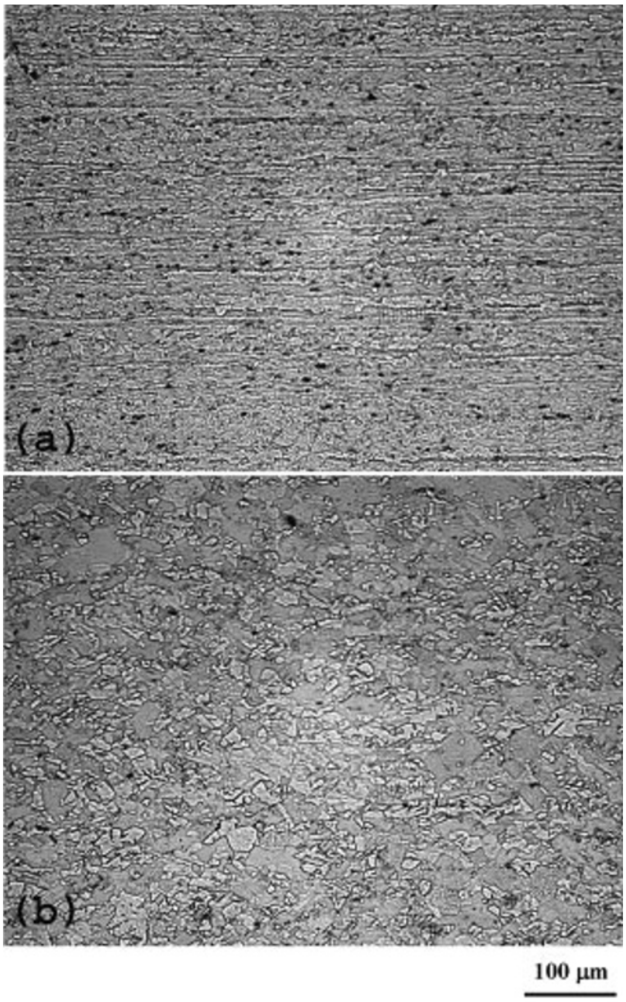


**Figure 1 – Microstructures of the base metals of (a) Aluminium, (b) Copper**

aluminium plate to the specified pin depth and then forcibly traversed along the joint line until the end of the weld was reached. The welding tool was then retracted while the tool continued to turn.

Surfaces for the observations of microstructure were etched by 1 % HF aqueous solution to reveal the aluminium microstructure and subsequently by a solution composed of $NH_4OH$, $H_2O_2$, and water for the copper microstructure. The microstructure was observed with an optical microscope and scanning electron microscope (SEM) for closer observations.

A peel test was employed to estimate the fracture load of the obtained joint. Dimensions of the specimen for the peel test are shown in Figure 2. The displacement speed was 0.3 mm/s. X-ray diffraction analyses using Cu-K$\alpha$ were carried out to identify the phases formed on the fracture surfaces of joint after the peel test.

## 3 EXPERIMENTAL RESULTS AND DISCUSSION

### 3.1 Lap joint of aluminium to copper without intermediate layer

#### *3.1.1 Microstructure of joint*

The characteristic microstructures observed in Al-Cu joint directly bonded at a high rotation speed are shown

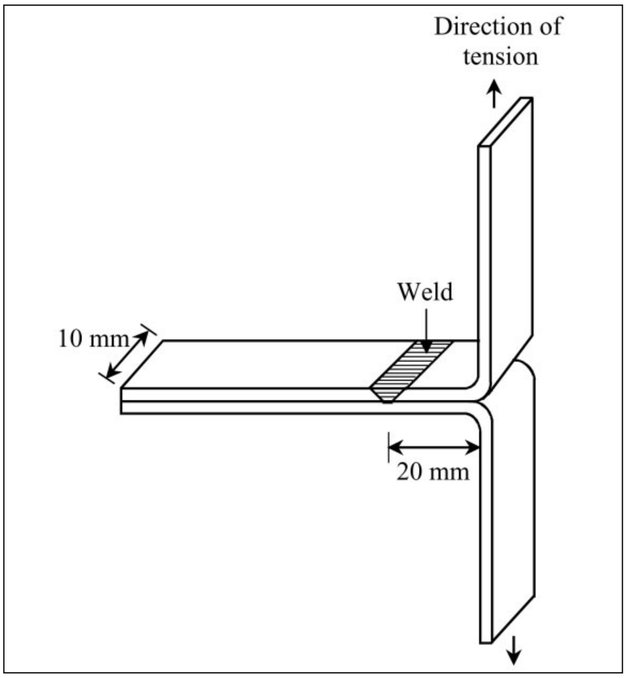


**Figure 2 – Schematic view of the specimen for peel test**

**Table 2 – Welding parameters and results from peel tests**

| Rotation speed $s^{-1}$ | Travel speed mm/s | Pin depth mm | Fracture Load N | | | Weld Number |
|---|---|---|---|---|---|---|
| | 3.3 | | 63.8 | 61.8 | 0 | 1 |
| 16.7 | 4.2 | | 57.9 | 74.6 | 62.8 | 2 |
| | 5 | | 0 | 0 | 0 | 3 |
| | 3.3 | | 96.1 | 113.8 | 254.1 | 4 |
| 25.0 | 4.2 | | 56.9 | 65.7 | 83.4 | 5 |
| | 5 | | 89.3 | 97.1 | 43.2 | 6 |
| | 3.3 | 2.1 | 156 | 154 | 186.4 | 7 |
| 33.3 | 4.2 | | 137.3 | 176.6 | 232.5 | 8 |
| | 5 | | 79.5 | 116.7 | 134.4 | 9 |
| | 3.3 | | 133.4 | 240.3 | 126.5 | 10 |
| 41.7 | 4.2 | | 170.7 | 155 | 238.4 | 11 |
| | 5 | | 94.2 | 277.6 | 161.9 | 12 |
| 33.3 | 3.3 | 2.2 | 526 | 482 | 487 | 13 |
| 41.7 | 3.3 | 2.2 | 501 | 461 | 491 | 14 |

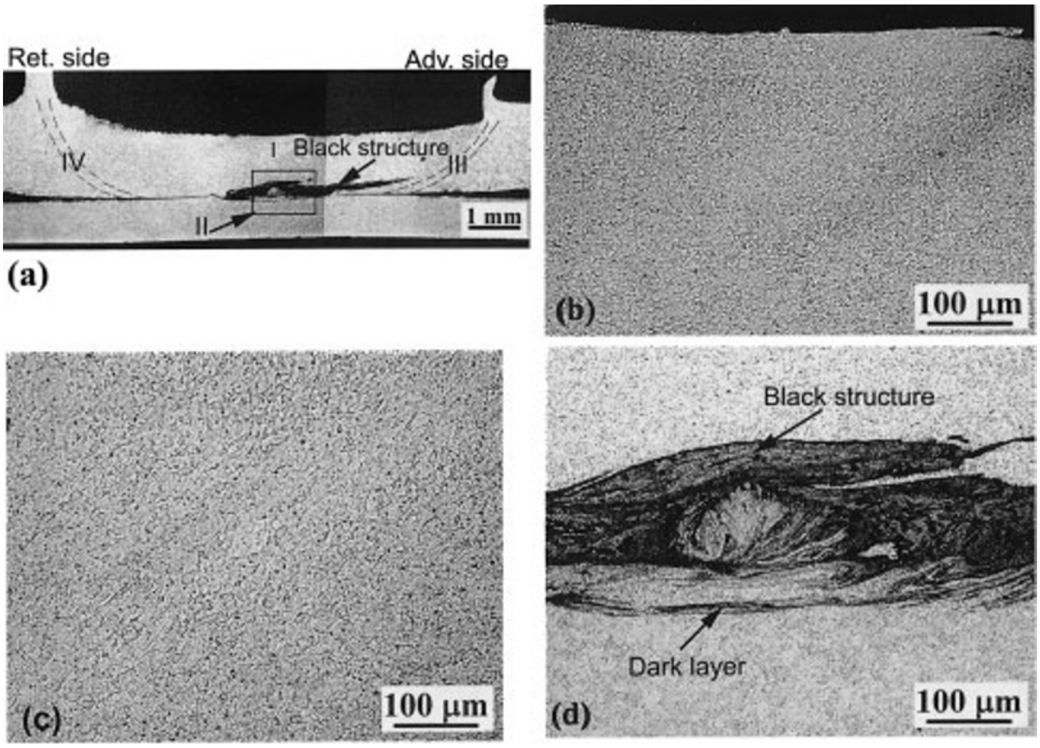


**Figure 3 – Characteristic microstructures of different areas in Al-Cu FSW**
**(a) Macrostructure of the joint, (b) Fine equiaxed grains zone (in stir zone) of aluminium (area I), (c) Aluminium HAZ on the advancing side (area III), (d) Al/Cu interface zone (area II)**

in Figure 3. More welding flash was released from the surface of the retreating side, where the direction of the tool rotation was opposite to the travel direction of the tool as shown in Figure 3 (a). Black microstructure was observed in the aluminium near the Al/Cu interface when the rotation speed was higher than 16.7 $s^{-1}$. This black structure extended toward the advancing side of the joints with increasing the travel speed to reach the aluminium surface at the highest travel speed.

The microstructure of the aluminium stir zone was characterized by equiaxed fine grains [area (I)] as shown in Figure 3 (b). Several authors suggested that the equiaxed fine grain in the stirred zone was formed through the dynamic recrystallisation followed by the static recrystallisation for a short period during the cooling process [19-21].

Between area (I) and the base metal of aluminium, narrow heat-affected zones (areas III and IV) were observed which were characterized by slightly coarser grains than those of the stir zone. The HAZ microstructure on the advancing side is shown in Figure 3 (c). In area (II), black structures were formed mainly in the aluminium close to the Al/Cu interface as shown in Figure 3 (d). The copper side was characterized by thin layers of dark structure very near to Al/Cu interface as shown in Figure 3 (d). This layer is different in colour from the black structure mentioned above and can be considered to be similar to the layer structure [see Figure 4 (a)] from chemical composition and microstructural features. It was also recognized that grains in the copper close to Al/Cu interface was finer than those of the copper base metal though not obviously observed in Figure 3 (d). This difference in the grain size can be

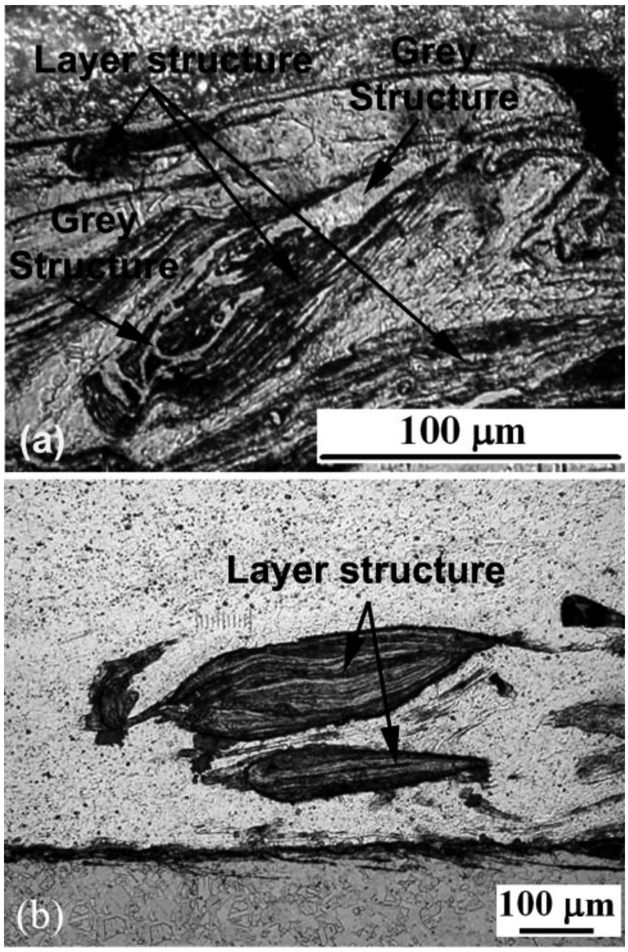


**Figure 4 – Microstructures formed in the area close to Al-Cu interface**
**(a) Layer and grey structures,**
**(b) Copper-rich fragment with layer structure**

attributed to the effect of rotating pin which deformed the grains close to Al/Cu interface.

The structure of the Al/Cu interface region was complicated. A layer structure which consisted of mechanically mixed Cu and Al rich layers was formed in the area close to the interface as shown in Figure 4 (a). It is noted that grey structure were accompanied by the layer structure as indicated in Figure 4 (a). Fragments of copper distributed randomly in the aluminium substrate near the interface with various size and structures [see Figure 4 (b)]. Some of the fragments contained the layer structure and the others contained fine grains of copper rich structure.

Thus, the characteristic microstructures observed in the directly bonded joint of an aluminium plate to copper plate were the black structure, grey structure, and layer structure. The results from EDX analyses of these microstructures are indicated in Figure 5, with overlapping the Al-Cu phase diagram. This suggests that all these microstructures consisted of or included intermetallic compounds of Al-Cu system.

### *3.1.2 Mechanical properties of joints*

The hardness distribution along the vertical axis to the weld is shown in Figure 6. The average hardness of the aluminium stir zone was 30 Hv. The black structure showed higher hardness depending on its copper content. Meanwhile, the hardness of the layer and fine grain copper structures were much higher than the other areas as shown in Figure 7.

The fracture load of the joint in peel test is shown in Table 2. Although the measured value of the fracture load was scattered quite widely, it showed a general tendency to slightly decrease by increasing the travel speed from 3.3 to 5 mm/s. Increasing the rotation speed from 16.7 to 41.7 $s^{-1}$ improved the fracture load.

For joints bonded at rotation speeds of 25.0 $s^{-1}$ to 41.7 $s^{-1}$, the fracture on peel test occurred along the path as observed in Figure 8 (a). Enlargement of some areas on copper side [Figure 8 (b) and 8 (c)] presented that the layer structure was covered with the grey structure. This suggested that the fracture occurred mainly at grey structure which can be regarded as an intermetallic compound from its chemical composition (see Figure 5).

SEM micrographs of the fracture surfaces corresponding to the crack path shown in Figure 8 are shown in Figure 9. The fracture surfaces consisted mainly of two types of morphologies: ductile fracture and brittle fracture which was much more prominent. From the observation of each part shown in Figure 8, the formation of the intermetallic compounds in the layer and grey structures can be considered to be a main factor causing the brittle fracture.

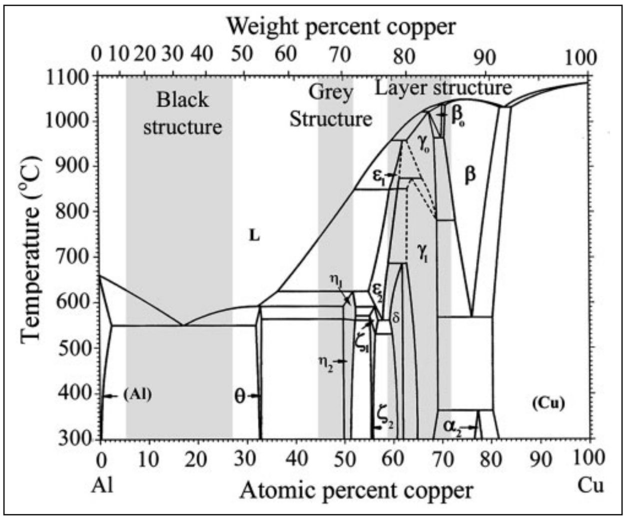


**Figure 5 – Compositions of black, grey, and layer structures in comparison with the Al/Cu phase diagram**

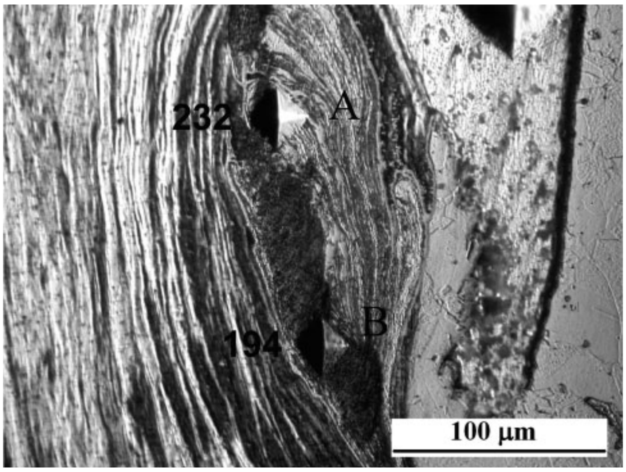


**Figure 7 – Hardness values of the layer structure, point A, and fine grain copper structures, point B, (weld No. 10)**

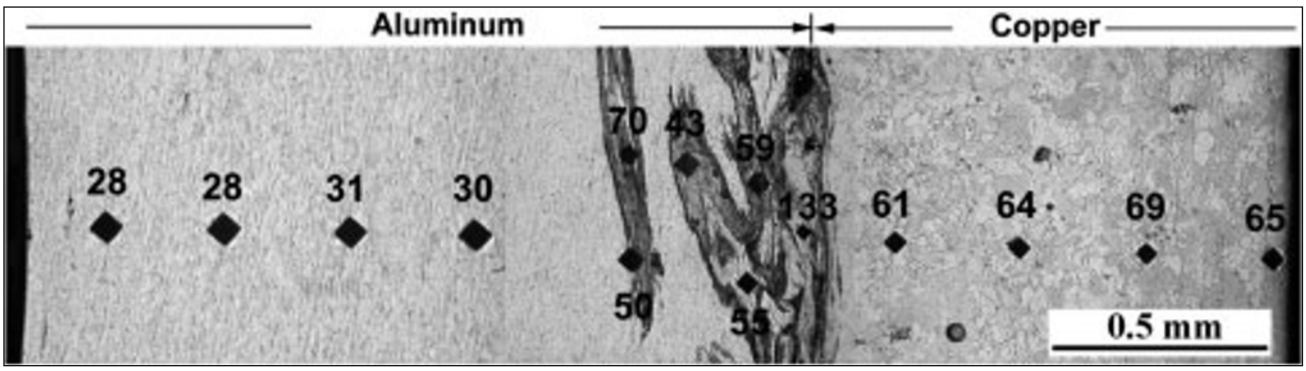


**Figure 6 – Hardness distribution (Hv0.49N) perpendicular to the Al-Cu joint (weld No. 10)**

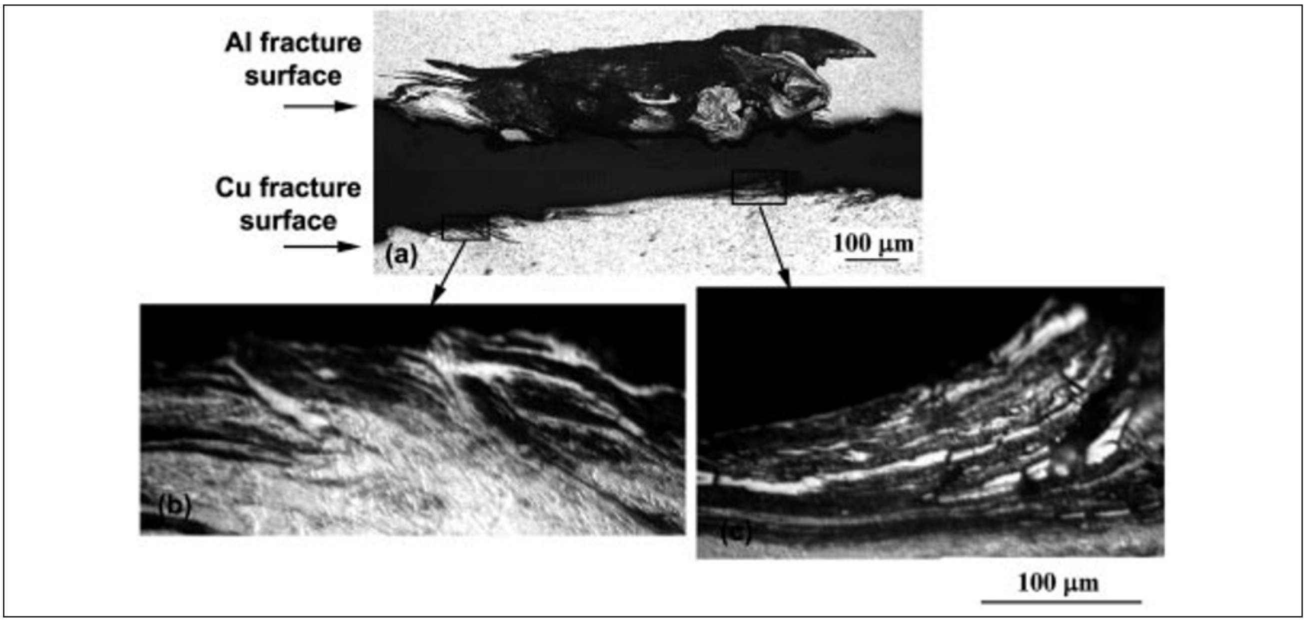


**Figure 8 – Cross sections of fracture surfaces (weld No. 12)**
**(a) Microstructure of the cross section, (b) and (c) Closer views of the rectangular area in (a)**

In order to identify the intermetallic compounds formed in the joint bonded at higher rotation speeds (25.0-41.7 $s^{-1}$), X-ray diffraction patterns from fractured surfaces of the aluminium and copper sides were analyzed as shown in Figures 10 (a) and 10 (b). As can be seen from these, intermetallic compounds of $Al_4Cu_9$, AlCu, and $Al_2Cu$ were detected from both aluminium side and copper side. This suggests that intermetallic compounds of $Al_4Cu_9$ and AlCu were formed in the grey and layer structures where the crack on the peel test was developed preferentially since these structures had Cu content more than 40 %.

## 3.2 Lap joint of aluminium to copper with zinc intermediate layer

### *3.2.1 Microstructure of joint*

The characteristic microstructures of the Al-Cu joints with zinc intermediate layer were similar to those observed in the joint welded without the intermediate layer except for some differences. The transverse sections of the joints observed at a low magnification are shown in Figure 11. The black structure in the joint with a Zn intermediate layer was limited in a narrower area than that observed in the joint without an intermediate layer. Thus the Zn intermediate layer interfered with the development of the black structure. One more important difference was the deeper penetration of the layer structure into the copper substrate owing to the greater penetration depth of the tool pin to the copper side as shown in Figure 12. In addition, the zinc layer was effective in obstructing the incorporation of Cu fragments into the aluminium stir zone in comparison with directly bonded (see Figure 12). It should be also mentioned that the grey structure formed in joints with a zinc intermediate layer was much thinner than those formed in directly bonded joints.

### *3.2.2 Mechanical properties of joints*

The hardness values of a joint welded with a zinc intermediate layer is shown in Figure 13. Although the layer structure showed the highest value, it was softer than those observed at the directly-bonded interface and extended to deeper depth in the Cu substrate. The lower

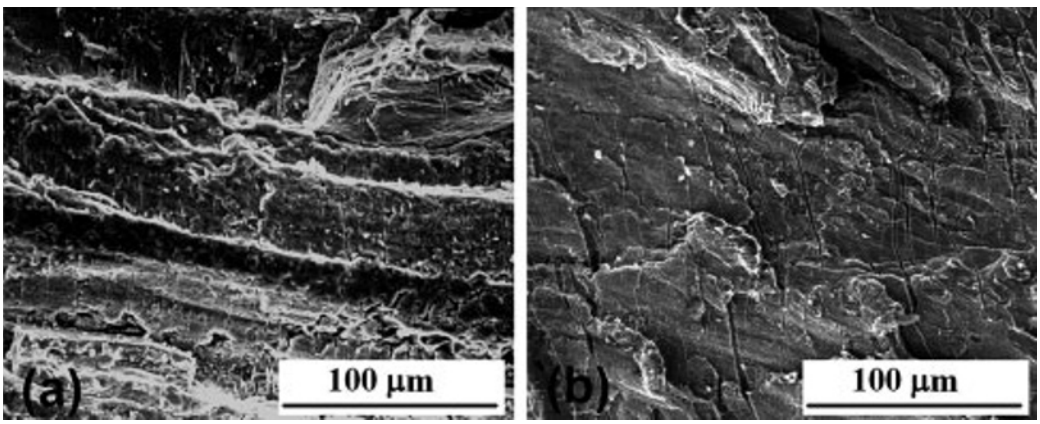


**Figure 9 – Fracture surfaces of a joint after a peel test (weld No. 11)**
**(a) Brittle morphology on the aluminium side, (b) Brittle morphology on the copper side**

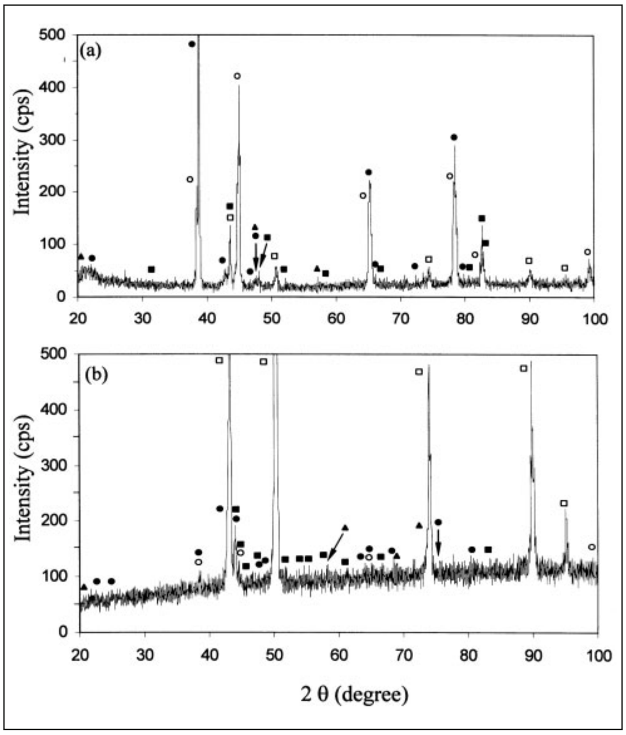


*The diffraction lines from aluminium, copper, $Al_4Cu_9$, AlCu, and $Al_2Cu$ were indicated by* ○, □, ●, ■, and ▲, respectively.

**Figure 10 – X-ray diffraction patterns from fracture surfaces (a) of the aluminium side, (b) of the copper side (weld No.10)**

hardness suggests that the different kinds of intermetallic compounds were involved in the layer structure, depending on the application of the Zn intermediate layer (see Figure 7).

The fracture load of the joint with a zinc intermediate layer was higher than that of directly-bonded joints under the same bonding condition. The average fracture load of the directly-bonded joint was 162 N, while the joint with a zinc intermediate layer achieved average fracture load of 491 N as shown in Table 2.

Not only were the fracture loads different between the joints bonded with and without a zinc intermediate layer, but also the path of the fracture. For the joint bonded directly without an intermediate layer, the fracture on peel test occurred along the path as shown in Figure 8. In contrast to this, the fracture of the join bonded with a zinc intermediate layer occurred along the path as shown in Figure 14. It should be noted that the joints bonded with a zinc intermediate layer was fractured mainly at

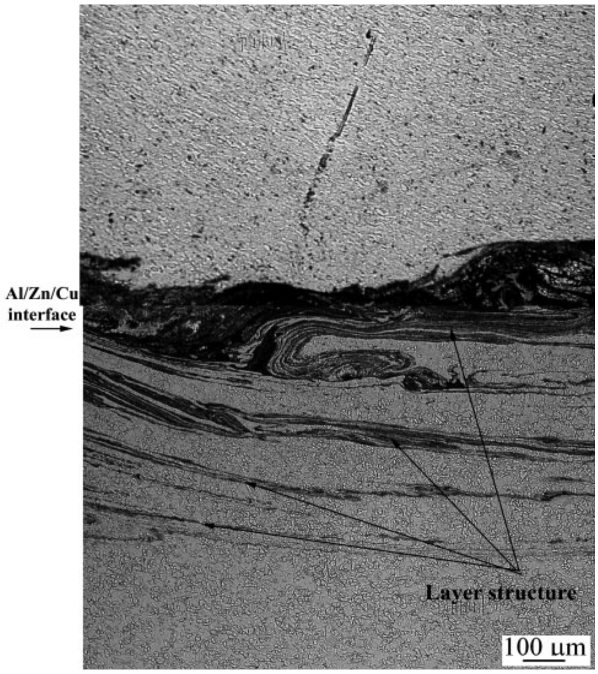


**Figure 12 – Penetration of layer structure in copper substrate**

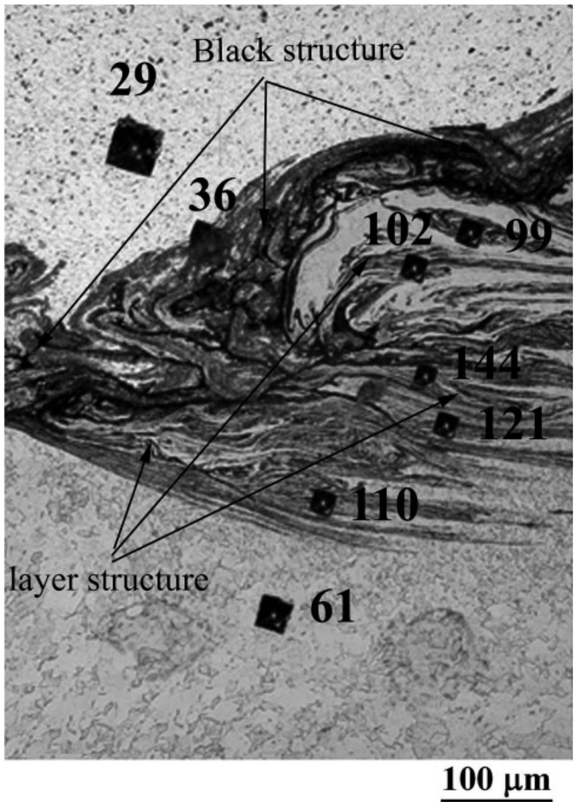


**Figure 13 – Hardness values at Al/Cu interface for Al-Cu joint with Zn intermediate layer**

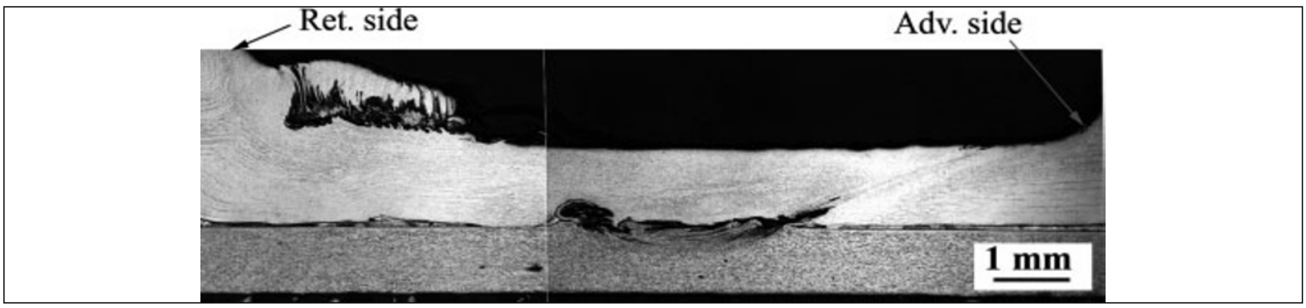


**Figure 11 – Macrostructure of the transverse sections of weld using Zn intermediate layer (weld No. 13)**

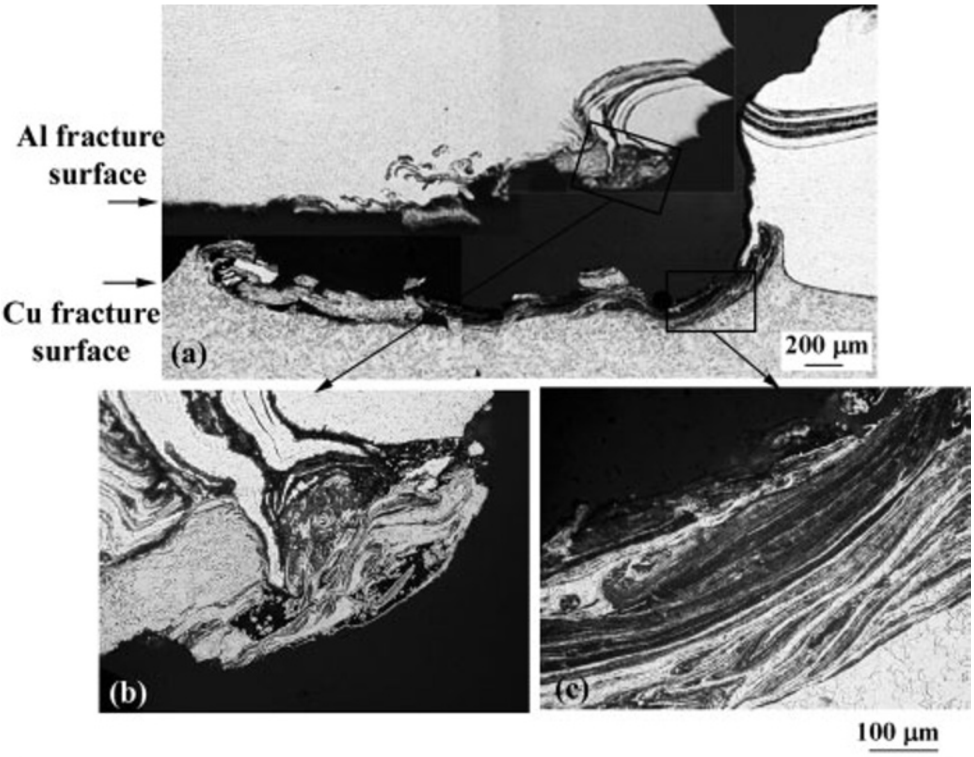


**Figure 14 – Cross sections of fracture surfaces**
**(a) Microstructure of the cross section, (b) and (c) Closer views of the rectangular areas in (a)**

the layer structure deeper in the copper substrate. This gives an indication that intermetallic compounds formed in the layer structure deeper in the copper substrate were more brittle than that formed at interface.

SEM micrographs of the fracture surfaces corresponding to the crack path shown in Figure 14 are presented in Figure 15. The area of ductile fracture increased to almost half of fracture surfaces, while brittle fracture was much more prominent for the directly bonded joint. The chemical analyses of the ductile area showed higher percentages of copper than the area of brittle fracture as shown in Table 3.

Mapping of Zn in the layer structures at Al/Zn/Cu interface was shown in Figure 16. It is obvious that the zinc content in the layer structure was decreased as it was away from the interface (see Figure 16). This suggests that the kinds of intermetallic compounds formed within the layer structure were changed with its distance from the interface.

X-ray diffraction patterns from fractured surfaces of the aluminium and copper sides were analysed. Although diffraction lines attributable to intermetallic compounds of $Al_4Cu_9$, AlCu, $Al_2Cu$, $CuZn_2$, $CuZn_5$ and $Cu_5Zn_8$ were detected from the aluminium and copper sides, those from Al-Cu intermetallic compounds were detected more from copper side, while those from Cu-Zn intermetallic compounds were detected more from aluminium side as can be seen from Figure 17. Probably these intermetallic compounds are less harmful and less brittle than Al-Cu intermetallic compounds. Therefore, the fracture path in the joints with a zinc intermediate layer was shifted to the copper side where more harmful Al-Cu intermetallic compounds were located.

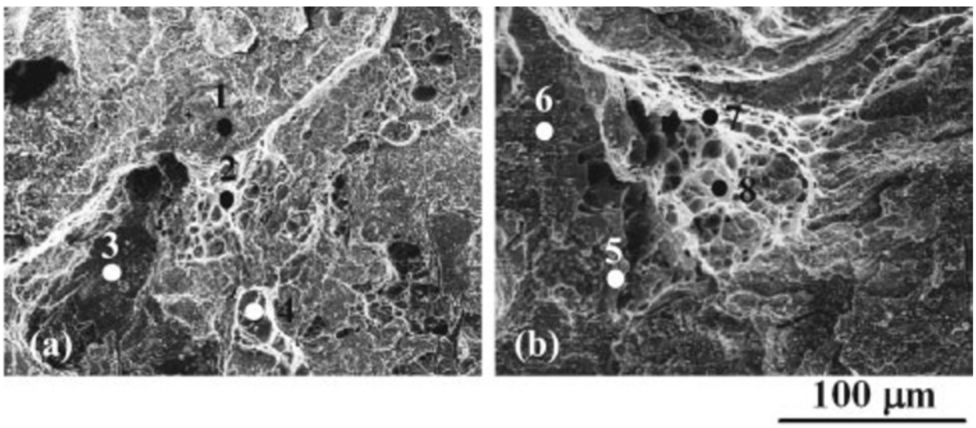


**Figure 15 – Fracture surfaces of a joint after a peel test (weld No. 11)**
**(a) and (b) Ductile/brittle morphology on Al and Cu sides respectively**

**Table 3 – Chemical analyses at points 1 to 8 indicated in Figure 15 (%)**

| Elements | Aluminium side | | | | Copper side | | | |
|---|---|---|---|---|---|---|---|---|
| | 1 | 2 | 3 | 4 | 5 | 6 | 7 | 8 |
| Al | 17 | 10 | 20 | 9 | 12 | 30 | 13 | 12 |
| Cu | 71 | 86 | 60 | 84 | 83 | 50 | 82 | 81 |
| Zn | 12 | 4 | 20 | 7 | 5 | 20 | 5 | 7 |

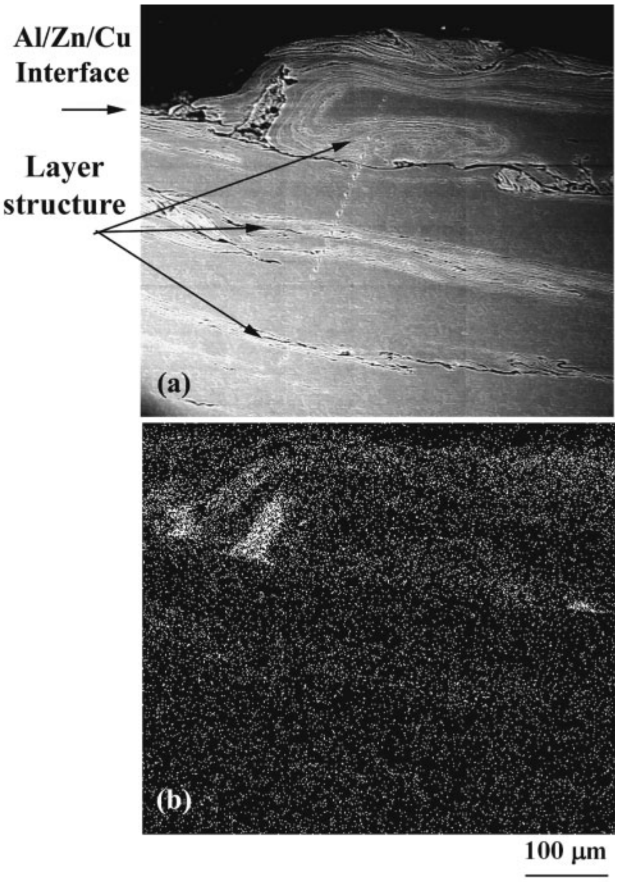


**Figure 16 – Mapping of Zn element in the layer structure at Al/Zn/Cu interface (a) Microstructure at the interface, (b) Mapping of Zn element**

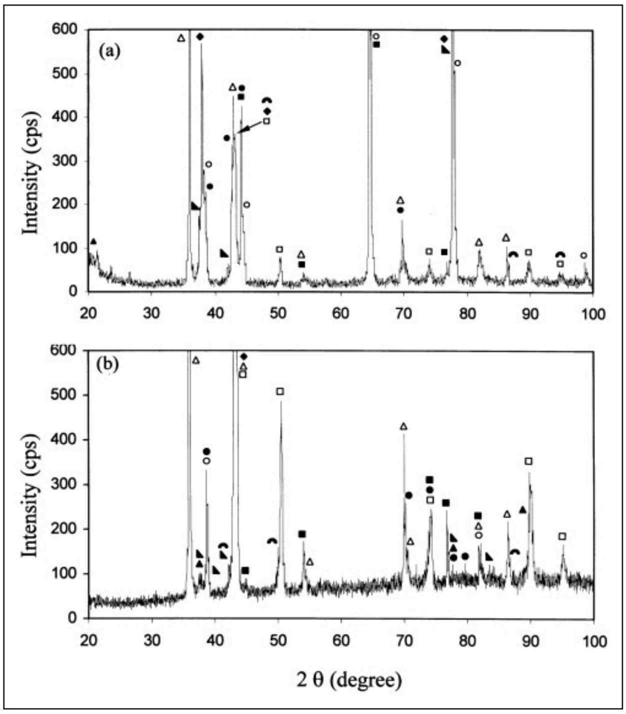


*The diffraction lines from aluminium, copper, zinc, $Al_4Cu_9$, AlCu, $Al_2Cu$, $CuZn_2$, $CuZn_5$ and $Cu_5Zn_8$ were indicated by ○, □, Δ, ●, ▲, ◆, ◣ and ∩, respectively.*

**Figure 17 – X-ray diffraction pattern from fracture surfaces (a) of the aluminium side, (b) of the copper side (weld No.13)**

These results suggest that mechanical properties of the FSW joint between aluminium and copper can be improved by using a zinc intermediate layer. Further improvements in the joint performance were expected by optimising the zinc layer thickness which will be our next trial to improve the joint performance.

## 4 CONCLUSION

**1.** The performance of lap joint of a commercially pure aluminium plate to a copper plate was improved significantly by using a zinc intermediate layer.

**2.** The characteristic microstructure of joints using a zinc intermediate layer were different from that of the joint directly bonded without an intermediate layer in respect to the limited formation of black and grey structure, the absence of the copper fragments incorporated into the aluminium substrate, and the deeper penetration of the layer structure into the copper substrate.

**3.** The average fracture load of joints with a Zn intermediate layer was almost three times as high as that of the joints bonded without an intermediate layer.

**4.** Joints with a Zn intermediate layer were fractured in ductile/brittle manner in the layer structures away from Al/Zn/Cu interface towards the copper substrate in comparison to the directly-bonded joints which fractured in brittle manner.

## REFERENCES

[1] Nakui S., Kawakami K., Ueoka T., Tsujino: Welding structure of metal specimens welded using ultrasonic welding systems with linear and complex vibration welding tips, WCU, 2003, Paris, September 7-10, pp. 1273-1274.

[2] Yilbas B.S., Sahin A.Z., Kahraman N., Al-Garni A.Z.: Friction welding of St-Al and Al-Cu materials, Journal of Metal Processing Technology, 1995, vol. 49, No. 3-4, pp. 431-443.

[3] Pinto M.A., Cheung N., Ierardi M.C.F., Garcia A.: Microstructural and hardness investigation of an aluminum-copper alloy processed by laser surface melting, Materials Characterization, 2003, vol. 50, No. 2-3, pp. 249-253.

[4] Lee W.B., Yeon Y.M., Jung S.B.: Joint properties of Friction stir welded AZ31B-H24 magnesium alloy Materials Science and Technology, 2001, vol. 19, pp. 785-790.

[5] Juhas M.C., Viswanathan G.B., Fraser H.L.: Microstructural evolution in a titanium alloy friction stir weld, Proc. Second Annual Symposium on Friction Stir Welding, Gothenburg, Sweden, June, 2000.

[6] Won-Bae Lee, Seung-Boo Jung: The joint properties of copper by friction stir welding, Material letters, 2004, No. 58, pp. 1041-1046.

[7] Thomas W.M., Threadgill P.L., Nicholas E.D.: Feasibility of friction stir welding steel, Science and Technology of Welding and Joining, 1999, vol. 4, No. 6, pp. 365-372.

[8] Lienert T.J., Stellwag W.L., Grimmett J.R.B.B., Warke R.W.: Friction stir welding studies on mild steel, Welding Journal, 2003, No. 1, pp. 1-9.

[9] Reynolds A.P., Wei Tang, Gnaupel-Herold T., Prask H.: Structure, properties, and residual stress of 304L stainless steel friction stir welds, Scripta Materialia, 2003, vol. 48, No. 9, pp. 1289-1294.

[10] Ying Li, Murr L.E., McClure J.C.: Flow visualization and residual microstructures associated with the friction-stir welding of 2024 aluminum to 6061 aluminum, Material Science and Engineering A, vol. 271, No. 1-2, 1999, pp. 213-223.

[11] Yoshikawa K., Harano T.: Numerically controlled friction stir welding in layered dissimilar metal materials of aluminum to steel, Proceedings of the third symposium on friction stir welding, Kobe, Japan, September 27-28, 2001.

[12] Takehiko W., Atsushi Y., Hirohumi T.: Bonding of steel and aluminum alloy by interfacial active adhesion bonding method -Interfacial active adhesion bonding of dissimilar material with a rotating needle, Preprints of the national meeting of J.W.S., 2002, No. 71, pp. 446-447, (in Japanese).

[13] Tsubaki M., Fukumoto M., Yasui T.: Evaluation of joining property between steel and aluminum by friction stirring, Preprints of the national meeting of J.W.S., spring 2003, No. 72, pp. 30-31, (in Japanese).

[14] Elrefaey A., Takahashi M., Ikeuch K.: Friction Stir Welding of Aluminum-to-Steel Lap Joint, 175th Meeting of the Technical Commission on Welding Metallurgy, JWS, Doc. WM-1891-04, Feb. 2004.

[15] Karlsson L., Berqvist E.L., Larsson H.: Application of friction stir welding to dissimilar welding, Annual assembly of IIW, Ljubljana, Slovenia, July 8-13, 2001.

[16] Murr L.E., Li Y., Flores R.D., Trillo E.A.: Intercalation vortices and related microstructural features in the friction-stir welding of dissimilar metals, Material Research Innovation, 1998, vol. 2, No. 3, pp. 150-163.

[17] Murr L.E., Flores R.D., McClure J.C., Liu G., Brown D.: Friction-stir welding: microstructral characterization, Material Research Innovation, 1998, vol. 1, No. 4, pp. 211-223.

[18] Elrefaey A., Takahashi M., Ikeuch K.: Preliminary investigation of friction stir welding aluminum/copper lap Joints, IIW Pre Assembly Meeting on FSW, Nagoya, Japan, July 2004, pp. 275-285.

[19] Sato Y.S., Kokawa H., Ikeda K., Enomoto M., Jogan S., Hashimoto T.: Microtexture in the friction-stir weld of an aluminium alloy, Metallurgical and Metals Transactions A, 2001, vol. 32A, No. 4, pp. 941-948.

[20] Jata K.V., Semiatin S.L.: Continuous dynamic recrystallization during friction stir welding of high strength aluminum alloys, Scripta Materialia, 2000, vol. 43, No. 8, pp. 743-749.

[21] Su J.Q., Nelson T.W., Mishra R., Mahoney M.: Microstructral investigation of friction stir welded 7050-T651 aluminum, Acta Materialia, 2003, vol. 51, No. 3, pp. 713-729.